

A Combined Finite Volume Discontinuous Galerkin Approach for the Sharp-Interface Tracking in Multi-Phase Flow

Stefan Fechter and Claus-Dieter Munz

Abstract In this paper, a numerical method for the simulation of compressible two-phase flows is presented. The multi-scale approach consists of several components that allow to sharply resolve the discontinuous nature of multi-phase flow: A discontinuous Galerkin solver for the macroscopic scales of the flow, a micro-scale Riemann solver at the interface that supplies the necessary interfacial jump conditions, a ghost-fluid based coupling of the interfacial conditions to the flow, and a level-set interface tracking formalism. To be able to locally guarantee a sharp and stable resolution at the interface, a finite volume technique on an adaptive sub-cell refinement is applied. The capabilities of the method are demonstrated for a three-dimensional shock-droplet interaction problem.

1 Introduction

In many technical applications, multi-phase flows meet conditions such as high pressure environments and/or high velocities that prohibit the popular assumption of incompressibility. Important examples for such extreme ambient conditions include fuel injection systems of aeronautical, automotive and rocket engines that are used at high-pressure operating conditions. The numerical simulation of compressible multi-phase flow is much more difficult than the incompressible treatment, because all conservation equations are coupled via the equation of state (EOS) and have to be solved simultaneously in a consistent way. In the commonly used incompressible treatment hydrodynamics and thermodynamics are decoupled.

S. Fechter · C.-D. Munz (✉)
Institute of Aerodynamics and Gas Dynamics, University of Stuttgart,
Pfaffenwaldring 21, 70569 Stuttgart, Germany
e-mail: munz@iag.uni-stuttgart.de

S. Fechter
e-mail: fechter@iag.uni-stuttgart.de

Three elements are crucial for compressible multi-phase solvers: The first is a numerical method to cope with the large discontinuities in the flow field. The second is the sharp resolution of the interface and the determination of the proper interfacial conditions. Here, we apply a ghost-fluid method as in [2] and supply the interface jump conditions by local Riemann solvers [1]. The third includes the accurate description and tracking of the phase interface that allows for the localisation as well as an estimation of the interface curvature. Here, a level-set method [6] is chosen, as it is easily applicable in the context of high-order methods.

In Sect. 2 these building blocks of the numerical method are described. In Sect. 3 the shock droplet interaction problem is shown, followed by a short conclusion.

2 Building Blocks for Sharp Interface Tracking

To be able to include local interfacial phenomena such as surface tension or phase change into the flow simulation, a heterogeneous multi-scale approach is considered, which is based on the solution of the Riemann problem. In the following we neglect viscosity and consider, for simplicity, the Euler equations as macro scale model together with suitable equation of states for the accurate description of multi-phase flows.

The numerical solution of the macro-scale model is provided by a discontinuous Galerkin spectral element method (DGSEM) with an explicit time approximation as described in [3]. At the interface position a Riemann solution is calculated. In case of phase transition the usual solution of the Riemann problem, consisting of four constant states separated by simple waves, breaks down. Information from the micro scale has to be used to get a thermodynamical consistent approximation. With micro scale we denote information from smaller scales that are not resolved by the numerical scheme, e. g. from molecular theory at the interface. Hence, the coupling between the micro and macro scale model is done via such a solution of the Riemann problem. The sharp approximation of the interface is accomplished in the flow solver by shifting the interface always away from the grid cell boundary and calculating the numerical flux within the flow solver by the classical Riemann problem only. Note that this ghost-cell approach does not preserve the conservativity locally.

In the following we describe the basic steps of the sharp interface treatment:

- Step 1: Computation of the interfacial curvature based on the level-set solution.
- Step 2: Solution of the multi-phase Riemann problem at the interface, identified by the level-set function. The data of the Riemann solver is given by interpolated values before and behind the interface. The Riemann solver takes the interface curvature into account, allows a general equation of state, and in the case of phase transition the local solution is established by additional local information from the micro-scale, see [1]. We call this the micro Riemann solver. The local interface velocity is an additional output parameter of the micro Riemann solver, which is then used to describe the interface motion in the level-set equation.

- Step 3: The explicit DGSEM is used to advance the flow field to the next time level t^{n+1} . Via the ghost-cell approach the flow solver has only grid cells within the bulk phases and rely on standard Riemann solvers for general equation of state. The flux at the phase interface is given by the micro Riemann solver.
- Step 4: The new position of level-set zero is used to determine the new position of the interface. In case the interface has moved across a grid cell, the new state is extrapolated using the adjacent grid cells with the same fluid.
- Step 5: Based on the refinement indicator that takes the local level-set value as well as a Persson oscillation indicator into account, the refinement is updated.

These are the basic steps of the sharp interface treatment, which are explained in the following in more details.

2.1 The Discontinuous Galerkin Spectral Element Method

In this section we describe the discontinuous Galerkin spectral element method for the flow equations. The description of the method is kept short, for more details we refer to Hindenlang et al. [3].

The key properties of the method are the following. The three-dimensional domain is divided into non-overlapping hexahedral elements, each mapped onto a reference cube element $E := (-1, 1)^3$ by a mapping $\zeta(x)$. The conservation equations on this reference element read as

$$JU_t + \text{div } F(U) = 0 \tag{1}$$

with a flux $F(U) = (F^1(U), F^2(U), F^3(U))$ and with Jacobian J of the transformation onto the reference cube. The approximate solution has the form

$$U_h(t, \zeta) = \sum_{i,j,k=0}^N \hat{U}(t)_{ijk} \psi_{ijk}(\zeta), \quad \psi_{ijk}(\zeta) = l_i(\zeta^1)l_j(\zeta^2)l_k(\zeta^3), \tag{2}$$

where $l_j(\zeta)$ are 1D Lagrange polynomials of degree N defined as:

$$l_j(\zeta) = \prod_{\substack{i=0 \\ i \neq j}}^N \frac{\zeta - \zeta_i}{\zeta_j - \zeta_i}, \quad j = 0, \dots, N. \tag{3}$$

Here the points $\zeta_j, j = 0, \dots, N$ are the Gauss-Legendre or Gauss-Legendre-Lobatto points in the reference cube E . These points are named interpolation points, the basis is the corresponding tensor product basis, and $\hat{U}(t)_{ijk}$ are the time-dependent degrees of freedom. Multiplying (1) with a test function ϕ and integration by parts of the second term leads to three contributions: A volume integral of the

time derivative term (*a*), a surface integral term (*b*) and a volume integral term (*c*), which now contains the gradient of the test function ϕ :

$$\underbrace{\frac{\partial}{\partial t} \int_E J U_h \phi d\zeta}_a + \underbrace{\int_{\partial E} (F^* \cdot N) \phi dS}_b - \underbrace{\int_E F(U_h) \cdot \text{grad}(\phi) d\zeta}_c = 0. \quad (4)$$

Volume as well as surface integrals are approximated by Gauss-Legendre or Gauss-Legendre-Lobatto quadrature. Hence, the quadrature points coincide with the interpolation points. As no continuity constraint is enforced between the elements, the flux function $F(U)$ at the cell boundaries is replaced by a numerical flux function $F^*(U^-, U^+)$ depending on the left and right adjacent states U^- and U^+ .

In the Galerkin approach the test functions are identical to the basis functions $\phi = \psi_{ijk}$. All the integrals are split in the different coordinate directions and approximated by Gauss-Legendre (-Lobatto) quadrature, which introduces the integration weights $\omega_i, i = 0, \dots, N$. As the quadrature points are chosen to be the same as the interpolation points, the Lagrange property $l_j(\zeta_i) = \delta_{ij}; i, j = 0, \dots, N$ can be exploited. The final semi-discrete form of the DGSEM scheme reads as

$$\begin{aligned} (\hat{U}_{ijk})_t = & - (J_{ijk})^{-1} \left[- \sum_{\lambda=0}^N \frac{\omega_\lambda}{\omega_i} D_{i\lambda} F_{\lambda jk}^1 - \sum_{\mu=0}^N \frac{\omega_\mu}{\omega_j} D_{j\mu} F_{i\mu k}^2 - \sum_{\nu=0}^N \frac{\omega_\nu}{\omega_k} D_{k\nu} F_{ij\nu}^3 \right. \\ & + \left([F^* \hat{s}]_{jk}^{+\zeta^1} \frac{l_i(1)}{\omega_i} - [F^* \hat{s}]_{jk}^{-\zeta^1} \frac{l_i(-1)}{\omega_i} \right) + \left([F^* \hat{s}]_{ik}^{+\zeta^2} \frac{l_j(1)}{\omega_j} - [F^* \hat{s}]_{ik}^{-\zeta^2} \frac{l_j(-1)}{\omega_j} \right) \\ & \left. + \left([F^* \hat{s}]_{ij}^{+\zeta^3} \frac{l_k(1)}{\omega_k} - [F^* \hat{s}]_{ij}^{-\zeta^3} \frac{l_k(-1)}{\omega_k} \right) \right]. \end{aligned}$$

The numerical fluxes F^* are evaluated at the faces of the reference element in each coordinate direction. These terms are denoted by $[\]^{-\zeta^1}$ and $[\]^{+\zeta^1}$ for the left and right face in ζ^1 -direction and analogously for ζ^2 and ζ^3 . With $D_{ij} = dl_j(\zeta)/d\zeta|_{\zeta=\zeta_i}$ a differentiation matrix is denoted, which is needed for the integrand of the volume integral. This semi-discrete formulation is then approximated in time by an explicit fourth-order Runge-Kutta scheme.

2.2 Adaptive Mesh Refinement (AMR) and Finite Volume Subcells

The advantage of the DG scheme is that high-order approximations can be applied on coarse grids, which is very efficient with respect to the computational effort. With this approach difficulties occur at any discontinuity as e.g. at a phase interface. The continuous in-cell resolution of the DG scheme is not favorable to resolve jump at the phase interface. Our approach to overcome this problem is to replace the coarse DG grid cells by multiple subcells on which a second-order finite volume scheme is applied in the vicinity of the phase interface. The subcell refinement is done such that the number of the degrees of freedom remain the same to avoid a negative impact

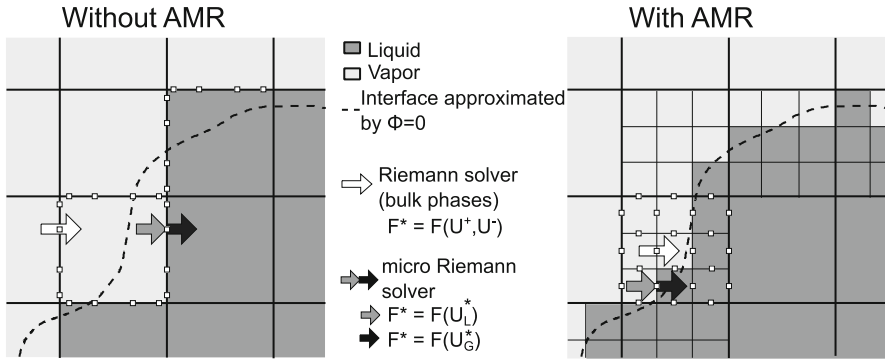


Fig. 1 Schematic representation of a typical setting in our sharp interface approach, involving the liquid-vapor interface, approximated by the zero level-set $\Phi = 0$, the computationally approximated computational interface aligned with the element boundaries and the different ways to apply the numerical fluxes provided by either a standard Riemann solver (bulk phase) or the micro Riemann solver at the computational interface. The white dots visualize the surface integration points

to the global time step restriction. The refinement and the flux calculation at the interface are visualized in Fig. 1 by showing the difference in the interface resolution with and without use of finite volume subcells.

This approach can be efficiently included into the DGSEM description. The coarse grid cell is now considered as a subdomain, in which a finite volume scheme is applied. The coupling to the neighbors is simply the weak coupling of the DG approach. Inside the grid cell the spectral scheme is replaced by a finite volume scheme on the sub-grid. The subcell ansatz enters the DGSEM description (4) in terms of a modified volume integral only. Instead of the continuous DG volume integral we calculate the sum of surface contributions for the equidistant subcell FV cells. This can be written in the following way

$$\int_E F(U) \cdot \text{grad}(\phi) \, d\zeta = \sum_{i,j,k=1}^N \int_{\partial e} \tilde{F} \cdot \tilde{n}_\xi \, dS, \tag{5}$$

where ∂e is the surface area of the subcell FV-cell e . This approach allows discontinuities between each subcell as no continuity constraint is enforced. At the interface between DG and FV cells, a conservative flux projection and interpolation method is chosen.

2.3 The Level-Set Interface Tracking Method

For interface tracking an additional conservation equation is solved. The level-set advection equation as introduced by Sussman [6] is recast to a conservation equation. This is done to be able to solve this equation with the DGSEM allowing for a high

order approximation. As compressible flow is considered here, an additional right-hand side term has to be solved that can be estimated using the high-order ansatz polynomials

$$\frac{\partial \Phi}{\partial t} + \operatorname{div}(s_{\text{PB}} \Phi) = \Phi \operatorname{div}(s_{\text{PB}}) . \quad (6)$$

The level-set distribution is solely important within a small region around the interface, where geometry and the secondary interface quantities are needed. Outside this region only the sign of the level-set function is important but not the magnitude. A narrow-band approach is used for the advection of the level-set function Φ .

Every 50–100 iterations (depending on the problem), the level-set is redistanced to a signed distance function to be able to accurately estimate the curvature κ (second derivative of the level-set function). This procedure resets the level-set function to a numerically preferable shape. The used algorithm is based on the constrained level-set reinitialization equation [6] that is discretized with a 5th order WENO scheme as described by Jiang and Peng [5].

For an accurate estimation of the curvature, the discontinuous Galerkin level-set solution is reconstructed using a $P_n P_m$ method to a polynomial of $M = 3N$. This is done to enhance the accuracy of the curvature calculation. The reconstruction reduces the negative impact of the discontinuous states at the element boundaries and allows for a element-local gradient estimation.

2.4 Coupling at the Phase Interface

The consistent numerical and thermodynamic approximation of the phase interface is provided by the solution of an approximate Riemann problem as described in [1]. The used linearized Lax curve Riemann solver has comparatively low computational costs and solely needs an estimation of the sound speed in both bulk phases at the interface. The effects of phase transfer can be included into the Riemann solution as described by Zeiler and Rohde in [7] for the isothermal case.

Surface tension effects are taken into account by a pressure jump according to the Young-Laplace law, for which the mean curvature at the interface is needed as input parameter. The user interface approximation is based on the use of non-conservative fluxes to ensure a sharp interface at all times. The interface propagation velocity s_{PB} is an additional output parameter and this approach allows for a more general treatment of the interface.

3 Computational Results

We show the capabilities of the numerical method by a shock-droplet interaction problem. The equation of state of a perfect gas is applied in the gaseous phase, while the Tait equation is used in the liquid phase. The initial conditions of the

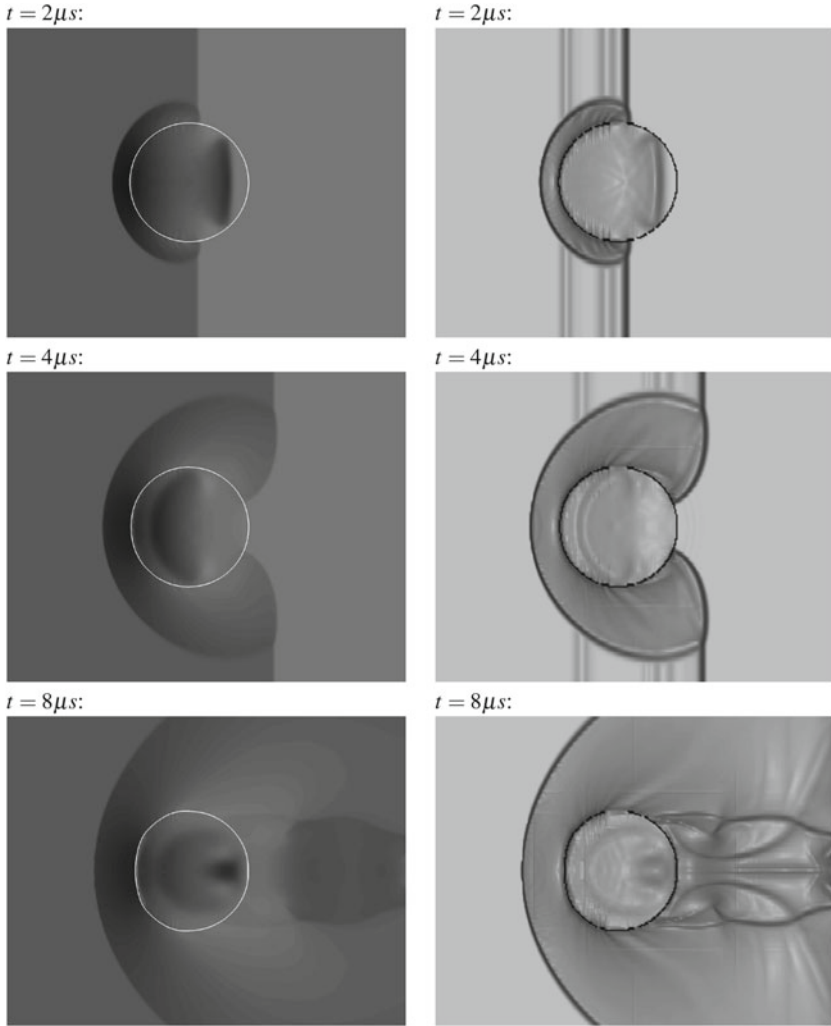


Fig. 2 Result of a 3D water droplet interacting with a planar shock at various time instances. *Left* pressure contours in the range of -20 to 40 atm. The *solid white line* indicates the interface position. *Right* Schlieren type image of the logarithmic density gradient $\log(\nabla\rho + 1)$

pre- and post-shock states are chosen according to Hu [4] featuring a $Ma = 3$ shock wave impacting on a initially spherical droplet. We consider here a three-dimensional shock-droplet interaction problem. At the domain boundaries in y and z -direction a wall boundary condition is assumed. The droplet's initial position is $(0.55, 0, 0)$, the initial position of the planar $M = 3$ shock is set to $x = 0.35$ inside a computational domain that extends $(0, -0.7, -0.7) \times (1.2, 0.7, 0.7)$. The non-dimensional parameters as described by Hu [4] are used in this test case. The chosen

numerical resolution was $80 \times 90 \times 90$ grid cells in the respective axis directions with a DG approximation of order four.

A Persson indicator based on the density is used for shock capturing purposes, which reliably detects the shock position. Depending on the indicator value, the time update is calculated using the fourth order accurate DG scheme in smooth regions or otherwise the TVD stable second order finite-volume scheme, which copes with strong discontinuities and shocks.

The results for simulation times of 2, 4 and $8 \mu\text{s}$ are shown in Fig. 2 in terms of a pressure plot and a Schlieren-type density gradient visualization. The introduced deformations of the droplet as well as the pressure and density-gradient visualization are in agreement to the reference simulations of Hu [4]. They conducted a higher resolved 2D simulation of the problem whereas here a slightly lower resolved 3D problem is considered.

4 Conclusion

In this paper, we introduced a numerical method for compressible two-phase flows using a sharp interface method. We applied the method to the simulation of a three-dimensional shock-droplet interaction. The present numerical approach allows for high order of accuracy as well as efficient calculations. The high order is especially advantageous in smooth parts of the flow and for the resolution of the interface as well as its curvature within the level-set approach. The sharp resolution of the interface is established by ideas from the ghost-fluid approach, adapted to the discontinuous Galerkin framework. At the interface the solution of a two-phase Riemann problem is used to get information about the interface states and propagation velocity.

References

1. Fechter, S., Jaegle, F., Schleper, V.: Exact and approximate Riemann solvers at phase boundaries. *Comput. Fluids* **75**, 112–126 (2013)
2. Fedkiw, R.P., Aslam, T., Merriman, B., Osher, S.: A non-oscillatory Eulerian approach to interfaces in multimaterial flows (the ghost fluid method). *J. Comput. Phys.* **152**(2), 457–492 (1999)
3. Hindenlang, F., Gassner, G., Altmann, C., Beck, A., Staudenmaier, M., Munz, C.D.: Explicit discontinuous Galerkin methods for unsteady problems. *Comput. Fluids* **61**, 86–93 (2012)
4. Hu, X.Y., Adams, N.A., Iaccarino, G.: On the HLLC Riemann solver for interface interaction in compressible multi-fluid flow. *J. Comput. Phys.* **228**(17), 6572–6589 (2009)
5. Jiang, G.S., Peng, D.: Weighted ENO schemes for Hamilton-Jacobi equations. *SIAM J. Sci. Comput.* **21**(6), 2126–2143 (2000)
6. Sussman, M., Smereka, P., Osher, S.: A level set approach for computing solutions to incompressible two-phase flow. *J. Comput. Phys.* **114**(1), 146–159 (1994)
7. Zeiler, C., Rohde, C.: A relaxation Riemann solver for compressible two-phase flow with phase transition and surface tension (2013)